

Analytical solutions for the Rabi model

Lixian Yu,^{1,2,3} Shiqun Zhu,¹ Qifeng Liang,² Gang Chen,^{3,*} and Suotang Jia³

¹*School of Physical Science and Technology, Soochow University, Suzhou, Jiangsu 215006, P. R. China*

²*Department of Physics, Shaoxing University, Shaoxing 312000, P. R. China*

³*State Key Laboratory of Quantum Optics and Quantum Optics Devices, Laser spectroscopy Laboratory, Shanxi University, Taiyuan 030006, P. R. China*

The Rabi model that describes the fundamental interaction between a two-level system with a quantized harmonic oscillator is one of the simplest and most ubiquitous models in modern physics. However, this model has not been solved exactly because it is hard to find a second conserved quantity besides the energy. Here we present a unitary transformation to map this unsolvable Rabi model into a solvable Jaynes-Cummings-like model by choosing a proper variation parameter. As a result, the analytical energy spectrums and wavefunctions including both the ground and the excited states can be obtained easily. Moreover, these explicit results agree well with the direct numerical simulations in a wide range of the experimental parameters. In addition, based on our obtained energy spectrums, the recent experimental observation of Bloch-Siegert in the circuit quantum electrodynamics with the ultrastrong coupling can be explained perfectly. Our results have the potential application in the solid-state quantum information processing.

PACS numbers: 42.50.Pq

I. INTRODUCTION

The Rabi model, which was introduced over 70 years ago, describes the important interaction between a two-level system and a quantized harmonic oscillator (bosonic mode) [1]. The corresponding Hamiltonian of this model is written as

$$H_R = \omega a^\dagger a + \frac{1}{2}\Omega\sigma_z + g\sigma_x(a^\dagger + a), \quad (1)$$

where a^\dagger and a are creation and annihilation operators for the quantized harmonic oscillator with frequency ω , σ_i ($i = x, y, z$) are the Pauli spin operators, Ω is the resonant frequency between two levels, and g is the interaction strength. In modern physics ranging from quantum optics [2], condensed-matter physics [3] to quantum information [4], the Rabi model has been one of the simplest and most ubiquitous models. Despite its old age and central importance, the Rabi model has not been solved exactly because it is hard to find a second conserved quantity besides the energy. The well-known method to obtain the energy spectrums and the wavefunctions for the Rabi model is the numerical diagonalization in a truncated finite-dimensional Hilbert space [5]. However, these numerical results are difficult to extract the fundamental physics of the Rabi model [6–12] and to precisely control the experimental parameters to process quantum information [13].

To overcome the problem in the analytical considerations, the rotating-wave approximation, which is valid in the regime $g \ll \omega$, was proposed to rewrite Hamiltonian

(1) as [14]

$$H_{JC} = \omega a^\dagger a + \frac{1}{2}\Omega\sigma_z + g(\sigma_- a^\dagger + \sigma_+ a). \quad (2)$$

Interestingly, the Jaynes-Cummings model with $U(1)$ symmetry has a conserved quantity $C = a^\dagger a + \frac{1}{2}(\sigma_z + 1)$, and thus, it can be solved easily in the subspaces $\{|\uparrow, n\rangle, |\downarrow, n+1\rangle\}$. Meanwhile, the Jaynes-Cummings model can successfully describe quantum dynamics of optical cavity electrodynamics with strong coupling. However, in the recent investigations about the solid-state quantum electrodynamics with the ultrastrong coupling ($g \sim 0.1\omega$) [15–24], the rotating-wave approximation breaks down and the system's dynamics must be governed by the Rabi model. Irish put forward a generalized rotating-wave approximation to solve the Rabi model. This method can be used to derive the analytical energy spectrums of Hamiltonian (1) in the ultrastrong coupling successfully [25]. However, this method works reasonable only for the negative detuning ($\Omega < \omega$) [26–28]. Recently, Braak used the property of Z_2 symmetry of the Rabi model to obtain its analytical solutions, which are, however, dependent of the composite transcendental function defining through its power series in the interacting strength g and the frequency ω [29]. In our previous work, we put forward a generalized variational method to analytically obtain the ground-state energy of the Rabi model, which agrees well with the numerical simulation in all regions of the resonant frequency of the two-level system including the negative detuning ($\Omega < \omega$), the resonant case ($\Omega = \omega$), and especially the positive detuning ($\Omega > \omega$). Unfortunately, our introduced method cannot be used to consider the excited-state energy spectrum [30].

In this paper, we present a simple and straightforward method to solve the Rabi model in both ground and excited states. We first map the unsolvable Rabi model (1)

*Corresponding author: chengang971@163.com

into a solvable Jaynes-Cummings-like model by choosing a proper variation parameter, as shown in Section II. Thus, the analytical energy spectrums including the ground and the excited states are obtained in section III. These derived analytical results agree well with the direct numerical simulations in a wide range of the experimental parameters. Moreover, the recent experimental observation of Bloch-Siegert [20], which is just the energy shift of the level transition, in the circuit quantum electrodynamics with the ultrastrong coupling can be well explained. In section IV, the analytical wavefunctions and the corresponding experimentally-measurable physics quantities such as the mean photon number are derived. Also, the obtained mean photon number can agree well with the numerical simulation. Finally, some conclusions are remarked in Section V.

II. MAPPING INTO THE JAYNES-CUMMINGS-LIKE MODEL

When performing a rotation around the y axis, the Rabi model becomes

$$H_R = \omega a^\dagger a + \frac{\Omega}{2} \sigma_x - g(a^\dagger + a) \sigma_z. \quad (3)$$

Under a unitary transformation

$$U = \exp[\lambda \sigma_z (a^\dagger - a)] \quad (4)$$

with λ being the dimensionless parameter determined by the following calculations, an effective Hamiltonian is given by $H_E = U H U^\dagger$, namely,

$$H_E = H_1 + H_2 + H_3, \quad (5)$$

where

$$H_1 = \omega a^\dagger a - \lambda \omega \sigma_z (a^\dagger + a) + \omega \lambda^2, \quad (6)$$

$$H_2 = -g[\sigma_z (a^\dagger + a) - 2\lambda], \quad (7)$$

$$H_3 = \frac{\Omega}{2} \{ \sigma_x \cosh[2\lambda(a^\dagger - a)] + i \sigma_y \sinh[2\lambda(a^\dagger - a)] \}. \quad (8)$$

Since $\cosh(y)$ and $\sinh(y)$ are the even and odd functions respectively, the terms $\cosh[2\lambda(a^\dagger - a)]$ and $\sinh[2\lambda(a^\dagger - a)]$ can be expanded as

$$\cosh[2\lambda(a^\dagger - a)] = G_0(N) + G_1(N)a^{\dagger 2} + a^2 G_1(N) + \dots \quad (9)$$

$$\sinh[2\lambda(a^\dagger - a)] = F_1(N)a^\dagger - a F_1(N) + F_2(N)a^{\dagger 2} - a^2 F_2(N) + \dots, \quad (10)$$

where $G_i(N)$ ($i = 0, 1, 2, \dots$) and $F_j(N)$ ($j = 1, 2, \dots$) with $N = a^\dagger a$ are the coefficients that depend on the dimensionless parameter λ and the photon number n . In general, the multi-photon process is weak in the Rabi model [2]. It means that the terms of the high-order

terms for a and a^\dagger in Eqs. (9) and (10) can be eliminated. As a result, the effective Hamiltonian (5) reduces to the form

$$H_E = \omega a^\dagger a - (\lambda \omega + g) \sigma_z (a^\dagger + a) + \omega \lambda^2 + 2\lambda g + \frac{1}{2} \Omega \{ \sigma_x G_0(N) + i \sigma_y [F_1(N)a^\dagger - a F_1(N)] \}. \quad (11)$$

In the eigenstates of σ_x with $\sigma_x |\pm x\rangle = \pm |\pm x\rangle$, the Pauli spin operators become $\sigma_z \rightarrow -(\tau_+ + \tau_-)$ and $\sigma_y \rightarrow -i(\tau_+ - \tau_-)$, where $\tau_z = |+\rangle \langle +x| - |-\rangle \langle -x|$, $\tau_+ = |+\rangle \langle -x|$ and $\tau_- = |-\rangle \langle +x|$, and the effective Hamiltonian (11) turns into

$$H_E = \omega a^\dagger a + \omega \lambda^2 + 2\lambda g + \frac{1}{2} \Omega G_0(n) \tau_z + R_r (\tau_+ a + \tau_- a^\dagger) + R_{ar} (\tau_+ a^\dagger + \tau_- a), \quad (12)$$

where

$$G_0(n) = \langle n | \cosh[2\lambda(a^\dagger - a)] | n \rangle, \quad (13)$$

$$R_r = \lambda \omega + g - \frac{1}{2} \Omega f_1(m, n), \quad (14)$$

$$R_{ar} = \lambda \omega + g + \frac{1}{2} \Omega f_1(m, n) \quad (15)$$

with $f_1(m, n) = \frac{\langle m | F_1(N)a^\dagger | n \rangle / \sqrt{n+1}}{\langle n+1 | F_1(N)a^\dagger | n \rangle / \sqrt{n+1}}$. It is straightforward to calculate that $G_0(n) = \langle n | e^{2\lambda(a^\dagger - a)} + e^{-2\lambda(a^\dagger - a)} | n \rangle / 2 = \langle n | e^{2\lambda(a^\dagger - a)} | n \rangle = e^{-2\lambda^2} L_n(4\lambda^2)$ and $f_1(m, n) = f_1(n+1, n) = \langle n+1 | \sinh[2\lambda(a^\dagger - a)] | n \rangle = 2\lambda e^{-2\lambda^2} L_n^1(4\lambda^2) / (n+1)$, where $L_n(y)$ is the Laguerre polynomial and $L_n^1(y)$ is the associated Laguerre polynomial. Thus, if the dimensionless parameter λ is chosen as $\lambda \omega + g + \frac{1}{2} \Omega f_1(n+1, n) = 0$, namely,

$$(\lambda \omega + g) + \frac{\Omega \lambda}{n+1} e^{-2\lambda^2} L_n^1(4\lambda^2) = 0, \quad (16)$$

the effective Hamiltonian (12) becomes a Jaynes-Cummings-like model

$$H_E = \omega a^\dagger a + \omega \lambda^2 + 2\lambda g + \frac{1}{2} \Omega G_0(n) \tau_z + R_r (\tau_+ a + \tau_- a^\dagger), \quad (17)$$

where $R_r = 2(\lambda \omega + g)$. By means of Hamiltonian (17), the analytical energy spectrums and wavefunctions for the Rabi model can be obtained easily in the subspaces $\{|+\rangle, n\rangle, |-\rangle, n+1\rangle\}$.

Before proceeding, the solution of the dimensionless parameter λ in Eq. (16) should be analyzed since it has a crucial role in obtaining the explicit energy spectrums and wavefunctions. In general, the nonlinear equation (16) cannot be solved analytically. However, in the current experimental setup with the ultrastrong coupling

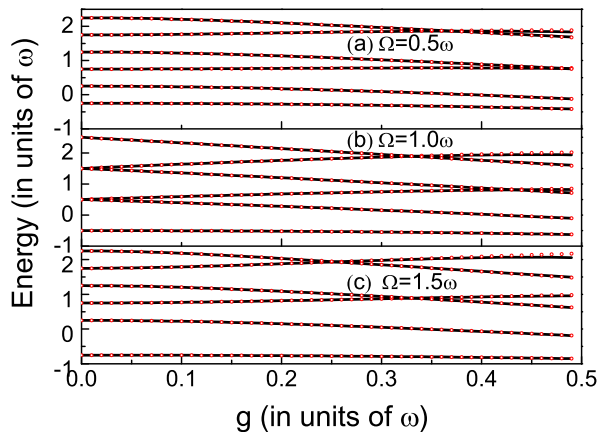


FIG. 1: (Color online) The energy spectrums of the ground and excited states for the Rabi model as a function of the interaction strength g for $\Omega = 0.5\omega$ (a), $\Omega = 1.0\omega$ (b), and $\Omega = 1.5\omega$ (c). The lowest line reflects the ground-state energy spectrum. In all figures, the black solid lines represent the exact numerical results, while the red open symbol corresponds to the analytical results obtained in the paper.

($g \leq 0.5\omega$), the numerical result shows that the dimensionless parameter λ is small compared with the unit. Thus, the associated Laguerre polynomial is given by $L_n^1(4\lambda^2) \simeq n + 1$ since $L_n^1(y) = n + 1 + \sum_{j>0} c_j y^j$, and Eq. (16) becomes $(\lambda\omega + g) + \Omega\lambda e^{-2\lambda^2} = 0$, which leads to a solution

$$\lambda \simeq -\frac{g}{\omega + \Omega \exp[-2(\frac{g}{\omega+\Omega})^2]}. \quad (18)$$

For the weak interaction strength g , the dimensionless

parameter becomes $\lambda \simeq -g/(\omega + \Omega)$.

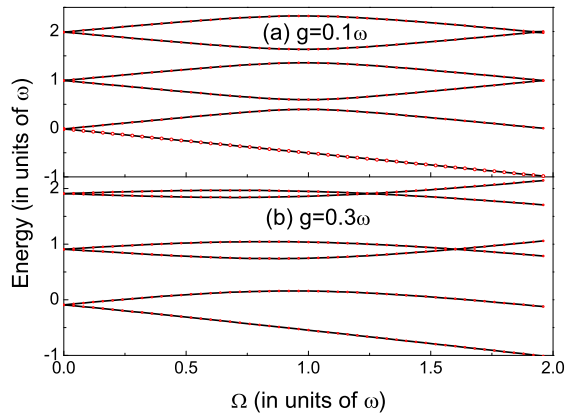


FIG. 2: (Color online) The energy spectrums of the ground and excited states for the Rabi model as a function of the resonant frequency Ω for $g = 0.1\omega$ (a) and $g = 0.3\omega$ (b). The lowest line reflects the ground-state energy spectrum. In all figures, the black solid lines represent the exact numerical results, while the red open symbol corresponds to the analytical results obtained in the paper.

III. ANALYTICAL ENERGY SPECTRUMS

In terms of the Jaynes-Cummings-like Hamiltonian (17) and Eq. (18), the ground-state energy spectrum can be written as

$$E_G = \omega\lambda^2 + 2\lambda g - \frac{1}{2}\Omega e^{-2\lambda^2}, \quad (19)$$

and the excited-state energy spectrum can be given by

$$E_{\pm, n} = (n + \frac{1}{2})\omega + \omega\lambda^2 + 2\lambda g + \frac{\Omega}{4}e^{-2\lambda^2} [L_n(4\lambda^2) - L_{n+1}(4\lambda^2)] \\ \pm \frac{1}{2} \sqrt{\{\omega - \frac{\Omega e^{-2\lambda^2}}{2} [L_n(4\lambda^2) + L_{n+1}(4\lambda^2)]\}^2 + 4[(\lambda\omega + g)\sqrt{n+1} - \frac{\Omega\lambda e^{-2\lambda^2}}{\sqrt{n+1}} L_n^1(4\lambda^2)]^2}. \quad (20)$$

The ground-state energy spectrum in Eq. (19) is identical to the result derived from the generalized variational method [30], which is, however, invalid for calculating the excited-state energy spectrum. In addition, for the weak resonant frequency Ω , Eqs. (19) and (20) reduce to the results obtained by means of the generalized rotating-wave approximation [25]. In Fig. 1, the energy spectrums of the ground and excited states for the Rabi model as a function of the interaction strength g for $\Omega = 0.5\omega$ (a), $\Omega = 1.0\omega$ (b) and $\Omega = 1.5\omega$ (c) are plotted, compared the explicit results in Eqs. (19) and (20) with the direct numerical simulation. This figure shows that our analytical energy spectrums including both the ground-

and excited states agree perfectly with the direct numerical simulation in the current experimental setup with the ultrastrong coupling ($g \leq 0.5\omega$). Moreover, these results are valid for all parameter regimes with the negative detuning ($\Omega < \omega$), the resonant case ($\Omega = \omega$), and especially the positive detuning ($\Omega > \omega$). This conclusion can be also drawn from Fig. 2, in which the energy spectrums as a function of the resonant frequency Ω for $g = 0.1\omega$ (a) and $g = 0.3\omega$ (b) are plotted. For the generalized rotating-wave approximation, the derived energy spectrums can agree well with the numerical simulation in the case of the negative detuning ($\Omega < \omega$). However, with the increasing of the resonant frequency Ω , this method

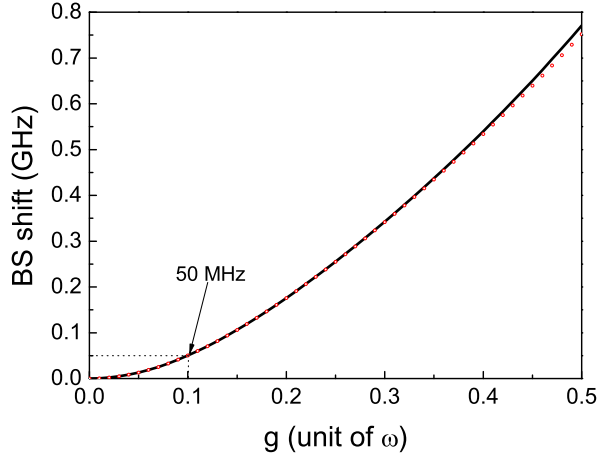


FIG. 3: (Color online) The Bloch-Siegert (BS) shift as a function of the interaction strength g with $\omega/2\pi = 8.13$ GHz and $\Omega/2\pi = 4.25$ GHz. In this figure, the black solid lines represent the exact numerical results, while the red open symbol corresponds to the analytical results obtained in the paper.

breaks down and the error is increased linearly.

In addition, by means of Eqs. (19) and (20), the Bloch-Siegert shift, which is just the energy shift of the level transition, can be also obtained. In Fig. (3), the smallest Bloch-Siegert shift with the transition $E_{-,0} \rightarrow E_G$ as a function of the interaction strength g is plotted. The other parameters are the same as those in the recent experiment of circuit quantum electrodynamics with the ultrastrong coupling [20], namely, $\omega/2\pi = 8.13$ GHz and $\Omega/2\pi = 4.25$ GHz. If $g/\omega = 0.1$, the smallest Bloch-Siegert shift is 50 MHz, which agrees well with the experimental observation [20].

IV. ANALYTICAL WAVEFUNCTIONS AND MEAN PHOTON NUMBER

The wavefunctions of the Rabi model (1) for the ground and excited states also need to be discussed. For the ground state, the corresponding wavefunction can be evaluated immediately as

$$|\varphi_0\rangle = e^{\frac{i\pi}{4}\sigma_y} e^{-\lambda\sigma_z(a^\dagger - a)} |0, -x\rangle. \quad (21)$$

For the excited state, the wavefunction for the Jaynes-Cummings-like Hamiltonian (17) is given by

$$\begin{cases} |+, n\rangle = \cos\theta_n |n, +x\rangle + \sin\theta_n |n+1, -x\rangle \\ |-, n\rangle = -\sin\theta_n |n, +x\rangle + \cos\theta_n |n+1, -x\rangle \end{cases}, \quad (22)$$

where

$$\theta_n = \frac{1}{2} \tan^{-1} \frac{2R_r}{E_{-,n} - E_{+,n}}, \quad (23)$$

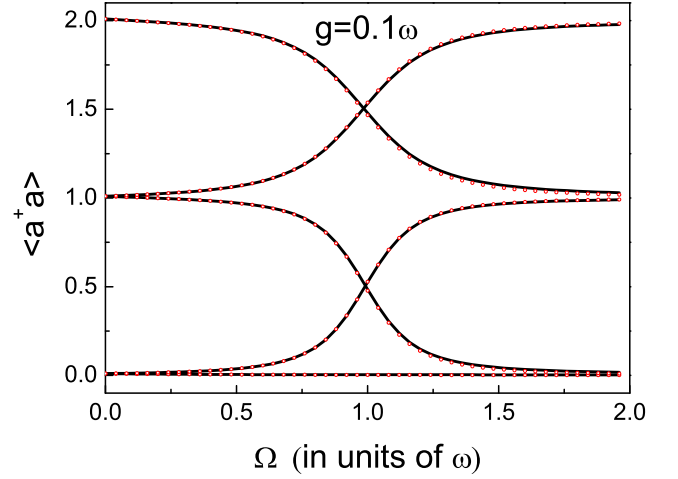


FIG. 4: (Color online) The mean photon numbers of the ground and excited states for the Rabi model as a function of the resonant frequency Ω for $g = 0.1\omega$. The lowest line reflects the ground-state mean photon number. In this figure, the black solid lines represent the exact numerical results, while the red open symbol corresponds to the analytical results obtained in the paper.

where $E_{\pm,n}$ are given by Eq. (20). Thus, the excited-state wavefunction for the Rabi model is given by

$$|\varphi_e\rangle = \begin{cases} e^{\frac{i\pi}{4}\sigma_y} e^{-\lambda\sigma_z(a^\dagger - a)} |-, m-1\rangle, & (m = 1, 3, \dots) \\ e^{\frac{i\pi}{4}\sigma_y} e^{-\lambda\sigma_z(a^\dagger - a)} |+, m-1\rangle, & (m = 2, 4, \dots) \end{cases}, \quad (24)$$

where m is the number of the excited state.

Based on the wavefunctions in Eqs. (21) and (24), the experimentally measurable physics quantities can be well derived. For example, the ground-state mean photon number can be given by $\langle a^\dagger a \rangle_0 = \langle \varphi_0 | a^\dagger a | \varphi_0 \rangle = \langle 0, -x | e^{\lambda\sigma_z(a^\dagger - a)} e^{-\frac{i\pi}{4}\sigma_y} a^\dagger a e^{\frac{i\pi}{4}\sigma_y} e^{-\lambda\sigma_z(a^\dagger - a)} |0, -x\rangle$, namely,

$$\langle a^\dagger a \rangle_0 = \lambda^2. \quad (25)$$

For the excited state, the mean photon number is given by

$$\langle a^\dagger a \rangle_e = \begin{cases} \mu + \lambda^2 + \frac{1+2\lambda \tan\theta_\mu \sqrt{m+1}}{1+\tan^2\theta_\mu}, & (m = 1, 3, \dots) \\ \nu + \lambda^2 + \frac{\tan^2\theta_\nu - 2\lambda \tan\theta_\nu \sqrt{m+1}}{1+\tan^2\theta_\nu}, & (m = 2, 4, \dots) \end{cases}, \quad (26)$$

where $\mu = (m-1)/2$ and $\nu = (m-2)/2$.

In Fig. 3, the mean photon numbers of the ground and excited states for the Rabi model as a function of the resonant frequency Ω for $g = 0.1\omega$ are plotted. This figure shows that the analytical results in Eqs. (25) and (26) agree well with the numerical simulation. It implies again that the effective Hamiltonian (17) can describe the current experimental setup with the ultrastrong coupling. Eq. (25) also shows that the ground-state mean photon number for the Rabi model depends on all parameters

including the frequency ω of the quantized harmonic oscillator, the interaction strength g , and especially, the resonant frequency Ω . It is quite different from the result derived from the generalized rotating-wave approximation that the ground-state mean photon number is independent of the resonant frequency Ω [25].

V. CONCLUSIONS

In summary, we have presented a unitary transformation to map the unsolvable Rabi model into a solvable Jaynes-Cummings-like model in the dress-state representation. As a result, the analytical energy spectrums and wavefunctions including both the ground and the excited states can be obtained easily. Moreover, our results agree perfectly with the direct numerical simulations in a wide

range of the experimental parameters and are valid for all regions of the resonant frequency of the two-level system including the negative detuning ($\Omega < \omega$), the resonant case ($\Omega = \omega$), and especially the positive detuning ($\Omega > \omega$). Our results can also explain the recent experimental observation in the circuit quantum electrodynamics with the ultrastrong coupling.

Acknowledgments

We thank Dr. Yuanwei Zhang for his helpful discussion. This work was supported partly by the 973 program under Grant No. 2012CB921603, the NNSFC under Grant Nos. 10934004, 60978018, 10904092, 11074154, 11074184 and 61008012, NNSFC Project for Excellent Research Team under Grant No. 61121064, and International Science and Technology Cooperation Program of China under Grant No.2001DFA12490.

-
- [1] I. I. Rabi, Phys. Rev. **49**, 324 (1936); **51**, 652 (1937).
 - [2] M. O. Scully, and M. S. Zubairy, *Quantum Optics* (Cambridge University Press, Cambridge, 1997).
 - [3] T. Holstein, Ann. Phys. (N.Y.) **8**, 325 (1959).
 - [4] J. M. Raimond, M. Brune, and S. Haroche, Rev. Mod. Phys. **73**, 565 (2001).
 - [5] Q. -H. Chen, Y. -Y. Zhang, T. Liu, and K. -L. Wang, Phys. Rev. A **78**, 051801 (2008).
 - [6] M. D. Crisp, Phys. Rev. A **43**, 2430 (1991).
 - [7] L. Lamata, J. León, T. Schätz, and E. Solano, Phys. Rev. Lett. **98**, 253005 (2007).
 - [8] H. Zheng, S. Y. Zhu, and M. S. Zubairy, Phys. Rev. Lett. **101**, 200404 (2008).
 - [9] R. Gerritsma, G. Kirchmair, F. Zähringer, E. Solano, R. Blatt, and C. F. Roos, Nature (London) **463**, 68 (2009).
 - [10] J. Larson, and S. Levin, Phys. Rev. Lett. **103**, 013602 (2009).
 - [11] J. Larson, Phys. Rev. A **81**, 051803 (2010).
 - [12] J. Larson, Phys. Rev. Lett. **108**, 033601 (2012).
 - [13] J. Q. You, and F. Nori, Nature (London) **474**, 589 (2011).
 - [14] E. T. Jaynes, and F. W. Cummings, Proc. IEEE **51**, 89 (1963).
 - [15] G. Günter, A. A. Anappara, J. Hees, A. Selll, G. Biasiol, L. Sorba, S. De Liberato, C. Ciuti, A. Tredicucci, A. Leitenstorfer, and R. Huber, Nature (London) **458**, 178 (2009).
 - [16] A. A. Anappara, S. D. Liberato, A. Tredicucci, C. Ciuti, G. Biasio, L. Sorba, and F. Beltram, Phys. Rev. B **79**, 201303, (2009).
 - [17] Y. Todorov, A. M. Andrews, R. Colombelli, S. De Liberato, C. Ciuti, P. Klang, G. Strasser, and C. Sirtori, Phys. Rev. Lett. **105**, 196402 (2010).
 - [18] M. Hofheinz, H. Wang, M. Ansmann, R. C. Bialczak, E. Lucero, M. Neeley, A. D. O'Connell, D. Sank, J. Wenner, John M. Martinis, and A. N. Cleland, Nature (London) **459**, 546 (2009).
 - [19] M. D. LaHaye, J. Suh, P. M. Echternach, K. C. Schwab, and M. L. Roukes, Nature (London) **459**, 960(2009).
 - [20] A. Fedorov, A. K. Feofanov, P. Macha, P. Forn-Díaz, C. J. P. M. Harmans, and J. E. Mooij, Phys. Rev. Lett. **105**, 060503 (2010).
 - [21] T. Niemczyk, F. Deppe, H. Huebl, E. P. Menzel, F. Hocke, M. J. Schwarz, J. J. Garcia-Ripoll, D. Zueco, T. Hümmer, E. Solano, A. Marx, and R. Gross, Nature Physics **6**, 772 (2010).
 - [22] B. Peropadre, P. Forn-Díaz, E. Solano, and J. J. García-Ripoll, Phys. Rev. Lett. **105**, 023601 (2010).
 - [23] M. Geiser, F. Castellano, G. Scalari, M. Beck, L. Nevou, and J. Faist, Phys. Rev. Lett. **108**, 106402 (2012).
 - [24] V. V. Albert, Phys. Rev. Lett. (accepted for publication).
 - [25] E. K. Irish, Phys. Rev. Lett. **99**, 173601 (2007).
 - [26] T. Liu, K. L. Wang, and M. Feng, EPL (Europhysics Letters) **86**, 54003 (2009).
 - [27] J. Hausinger, and M. Grifoni, Phys. Rev. A **82**, 062320 (2010).
 - [28] V. V. Albert, G. D. Scholes, and P. Brumer, Phys. Rev. A **84**, 042110 (2011).
 - [29] D. Braak, Phys. Rev. Lett. **107**, 100401 (2011).
 - [30] Y. Zhang, G. Chen, L. Yu, Q. Liang, J. -Q. Liang, and S. Jia, Phys. Rev. A **83**, 065802 (2011).